Thermo-Responsive Hydrogel-Coated Gold Nanoshells

Jun-Hyun Kim and T. Randall Lee*
Department of Chemistry
University of Houston,
Houston, TX, USA

***Abstract*-This manuscript describes the structural and optical properties of a new hybrid nanoparticle comprised of a gold shell/silica core structure (~120 nm in diameter) coated with an implantable hydrogel polymer overlayer (~20 nm in thickness). These nanoparticles are being developed as thermally modulated drug-delivery vehicles that respond to ambient changes in temperature. A unique feature of these materials is that the thermally sensitive hydrogel coatings can be modulated by exposure to light via excitation of the strong plasmon resonance of the gold shell/silica core particles. The gold nanoshell particles were tailored to absorb near-infrared light, which can pass readily through tissue and bone. The thermo-responsive hydrogel coating was prepared via radical polymerization of a selected mixture of N-isoproprylacrylamide and acrylic acid. The structure and morphology of the composite nanoparticles were examined by FE-SEM and TEM. UV-vis spectroscopy was used to characterize their optical properties, and DLS was used to determine their average hydrodynamic diameter as a function of temperature. As a whole, the results conclusively demonstrate that these composite nanoparticles can be reproducibly prepared, and their responses to changes in temperature are completely consistent with their use as nanoscale drug-delivery vehicles.**

***Keywords*—hydrogel, gold nanoshell, drug-delivery, hybrid nanoparticle, N-isopropylacrylamide, acrylic acid**

I. INTRODUCTION

Much recent work has been focused on the development of new types of nanostructured materials, such as nanorods, triangular prisms, disks, and nanoshells, for their use as new optical materials.[1–4] Certain strategies have attempted to transform initially prepared solid spheres into distinct shapes, while others have explored the use of shell/core architectures. The optical properties of the resulting nanostructured materials are strongly structure-dependent, often red-shifting and even separating the absorptions into distinctive dipole and quadrupole resonances.[5–6] Thus, these new nano-materials are being targeted for use in a variety of emerging electro-optical and biological applications.

Among metal nanoparticles, gold is readily biocompatible and widely used in the medical field.[7] As such, gold-based nanoparticles are particularly attractive nanomaterials for biological applications. The use of gold to coat dielectric core particles has received much attention not only because the resultant materials are expected to be biocompatible, but also because of their unique optical absorptions, which can be tailored across a wide range of wavelengths.[8] Gold nanoshells (GNSs) typically consist of a thin layer of gold around dielectric silica core.[9] Importantly, the size of the silica core and thickness of the gold shell can be specifically chosen during the preparation process to give particles with selected absorptions ranging from the visible to the near infrared.[10–11] Interestingly, light at wavelengths between 800 nm and 1200 nm, called the "water window", can penetrate human tissue and bone.[12] This specific range of wavelengths falls between the absorption of chromophores below 800 nm and that of water above 1200 nm.[12] It is also important to note that the absorption of light by GNS particles leads to rapid and efficient heating (*vide infra*).[13]

A specific goal of our research is to develop discrete biocompatible hydrogel-coated GNS particles that undergo structural changes from the heat generated by GNS core upon exposure to light. Hydrogel polymers are known to be key materials in a variety of technological applications, such as drug delivery, chemical separations, and catalysis.[14–16] In aqueous solution, hydrogels undergo volume transitions that depend on the lower critical solution temperature (LCST) and other chemical or physical stimuli.[17–19] Typical hydrogel polymers are hydrophilic and soluble in water below the LCST but become hydrophobic above that temperature.[20]

Various thermo-responsive hydrogel-based nanoparticles have been described in the literature, including those that incorporate poly(NIPAM).[21–24] Applications involving NIPAM homo-polymer hydrogels, however, are limited because thermally-induced structural changes occur at a fixed LCST of ~30 °C.[25] Researchers have overcome this limitation by incorporating acrylic acid (AAc) or acrylamide (AAm) into the hydrogel polymer matrix, which can shift the LCST of the hydrogel copolymers anywhere from ~30 to 60 °C.[26–27] The presence of AAc or AAm in the poly(NIPAM) backbone not only increases the LCST, but also causes the polymer to undergo reversible discontinuous volume changes in response to systematic variations in temperature.[26,28] Importantly, these copolymers form relatively thin surface layers that allow soluble materials held inside of the hydrogel particles to be released into the surrounding medium during the collapsing process.[28] It is our belief that these types of hydrogels can be coupled with GNS cores for use as drug-delivery carriers. Notably, the tunable optical properties of the GNS particles will enable these composite materials to become photothermally-responsive within the aforementioned "water window".

In the research described here, we adopted the technique of surfactant-free emulsion polymerization (SFEP)[29–31] to coat GNS particles with a thermo-responsive hydrogel polymer layer comprised of NIPAM-co-AAc. This strategy affords stable and chemically resistant hybrid nanoparticles that can be used to encapsulate organic and inorganic materials on the nanometer scale. As part of our long-term objective to prepare light-activated drug-delivery vehicles, this manuscript not only describes the preparation and characterization of these new nanoparticles, but it also demonstrates that the nanoparticles undergo well-behaved structural changes in response to external changes in temperature, offering a unique nanoscale delivery system that can be optically activated.

II. Experimental Section

A. Attachment of Gold Seed Particles to Amine-Functionalized Silica Particles

Silica core particles with a diameter of ~100 nm were prepared using a slight modification of the well known Stöber method.[32] Amine derivatization of the silica cores was effected using the method by Waddell *et al*., which employs excess APTMS.[33] The amine-functionalized silica particles were then centrifuged using an RC-3B Refrigerated Centrifuge (Sorvall Instruments) and redispersed in ethanol. Analysis by FE-SEM, TEM, and DLS showed no differences between the unfunctionalized and functionalized silica particles prepared in these experiments.

Gold seed particles were prepared using a modification of the method by Duff *et al*., which utilizes terakis(hydroxoy-methyl)phosphonium chlo-ride (THPC) as the reducing agent.[34–35] In our hands, the size of THPC gold seed particles could be precisely varied from 2–3 nm in diameter. It was necessary to store the solution of gold seeds in the refrigerator for at least three days to maximize the ability of the gold seeds to attach to the silica particle cores. The aged-THPC gold seeds were anchored onto the silica core particles using a modification of the Westscott *et al*. method.[36] The THPC gold seeds were deposited onto the silica particles by mixing 10 mL of the aged THPC gold solution (concentrated by a factor ranging from 0.1 to 0.2 after aging) with 1 mL of amine-functionalized silica nanoparticles overnight. The mixture was then centrifuged and redispersed in Milli-Q water, affording a solution that was light red in color.

B. Gold Nanoshell Growth[9]

A basic aqueous solution was prepared by mixing K_2CO_3 and $HAuCl_4 \cdot H_2O$ in water (K-gold solution). Specifically, 0.025 g of K_2CO_3 was completely dissolved in water by stirring, and then 2 mL of 1 wt% $HAuCl_4 \cdot H_2O$ was added to the mixture. The color of the solution quickly changed from yellow to colorless within 40 min and was stored in the refrigerator for one day without exposure to light.

To grow the gold shell on the gold-seeded silica core particles, 4 mL of the K-gold solution were placed in a 25 mL beaker with a stir bar, and 1.5 mL of the solution of the gold-seeded silica particles were added. These ratios afforded GNS particles with an absorption centered at ~850 nm. The mixture was stirred for at least 10 min, and then 0.02 mL of formaldehyde was added to reduce the K-gold solution. The color of the solution changed from colorless to blue, and the resultant GNS particles having a ~120 nm diameter (10 nm gold shell thickness) were purified by centrifugation. The precipitates were redispersed in Milli-Q water and used as a template for subsequent hydrogel growth.

C. Synthesis of Hydrogel-Coated GNS Particles

To prevent aggregation during the polymerization process, the GNSs were pre-washed with potassium carbonate solution. The hydrogel coatings were then grown by SFEP in aqueous solution. The GNS solution was diluted with Milli-Q water to give a maximum absorption of ~0.4 a.u. at 850 nm and placed in a three-necked round-bottomed flask equipped with a reflux condenser and an inlet for argon gas. An aliquot of 1.6 mL of degassed oleic acid (0.0017 mL; 6×10^{-6} mol) was then added to the stock solution under argon. The mixture was stirred for 1 h and sonicated for 15 minutes. An approximate 94:6 wt% ratio of NIPAM (0.04 g; 3.5×10^{-4} mol):AAc (0.0024 g; 3.3×10^{-5} mol) and the cross-linker BIS (0.004 g; 2×10^{-5} mol) were added to the mixture and stirred for 15 minutes. The mixture was then heated to 70 °C in an oil bath, and then the initiator APS (0.005 g; 2.2×10^{-5} mol) was added to promote the polymerization reaction, which was allowed to proceed for 8 h. The solution was cooled to room temperature and filtered through a 1 μm membrane to remove any micron-sized impurities and/or any aggregated particles. The filtered solution was centrifuged twice at 30 °C for 1 h at 3500 rpm, and the supernatant was separated to remove any unreacted materials and soluble side products. The purified nanoparticles were then diluted with Milli-Q water and stored at room temperature for later characterization. Analysis by DLS showed that the diameter of the hydrogel-coated GNS particles could be varied from ~160 nm to ~450 nm through minor variations in the amounts of monomer and initiator as well as the reaction time. We note, however, that the thickest hydrogel coatings were less reproducibly prepared than the thin coatings. We also found examples of multiple GNS cores within a single hydrogel shell in samples having the thickest hydrogel coatings. As such, we focused the bulk of our characterization efforts on hydrogel-coated GNS particles having ~160 nm diameters.

III. Results and Discussion

As described above, gold shells (~10 nm thick) were grown on silica cores (~100 nm diameter) to give particles with a strong absorption at 850 nm; these particles were then coated with a hydrogel jacket of thickness ranging from ~20 nm to ~165 nm. The polymerization onto the GNS particles was found to be convenient and reliable because all of the starting materials were readily soluble; even the GNS particles were well dispersed in the polymerization medium. This feature circumvented the need for any purification steps during the reaction. We caution, however, that phase separation can occur during the reaction if the polymerization conditions (e.g., temperature or monomer concentration) are varied widely. Notably, these composite nanoparticles are colloidally stable for more than two months at room temperature in aqueous solution.

Figure 1 shows FE-SEM images of the gold-seeded silica core particles, GNS particles, and hydrogel-coated GNS particles with both thin and thick coatings. We note first that there are no substantial differences in surface morphology between the gold-seeded silica particles (Figure 1a) and the bare GNS particles (Figure 1b); the diameters of the latter particles are, however, noticeably larger than those of the former. Figure 1b shows further that all of the GNS particles are homogeneous and monodisperse, which is a testament to the mono-dispersity of the ~100 nm diameter silica cores. Figure 1c highlights the marked optical contrast of the GNS cores and the hydrogel overlayers. Importantly, the contrast readily demonstrates the complete coating of the hydrogels around the GNS cores, the former appearing as halos around the bright centers. Similarly, Figure 1d illustrates the growth of substantially thicker hydrogel overlayers around the GNS cores. This image, however, also demonstrates a potential drawback of our methodology; namely, the encapsulation of multiple GNS particles within a single hydrogel polymer particle. This type of aggregation is rarely observed for the composites having thin hydrogel coatings. Precise control of this phenomenon is an ongoing research objective.

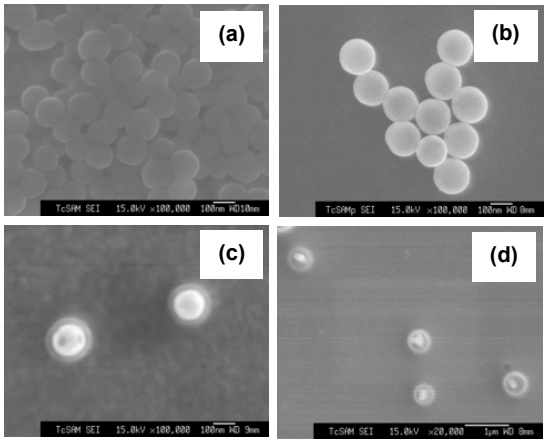

Figure 1. FE-SEM images of (a) THPC gold-seeded silica particles (~100 nm), (b) GNS particles (~120 nm), (c) thin hydrogel-coated GNS particles (~160 nm), (d) thick hydrogel-coated GNS particles (~450 nm).

Together with the FE-SEM images, we also collected EDX spectra of the hydrogel-coated GNS particles to characterize their elemental composition (spectra not shown). These measurements gave well-resolved peaks characteristic of gold (Mα and Lα at 2.12 and 9.71 keV, respectively) and silica (Kα and Kβ at 1.75 keV), but no peaks clearly attributable to the hydrogel polymer (as expected given the low atomic numbers of the constituent elements).

In separate studies, we used TEM to obtain high-resolution images of the hydrogel-coated GNS particles (see Figure 2). Because the polymer layer possesses low electron density, we selectively doped the AAc groups in the hydrogel polymer backbone through negative staining with 1% uranyl acetate in water to visualize the hydrogel coating on the GNS particles. In Figure 2b, the hydrogel layer appears as a thin halo surrounding the GNS core particle. As shown, these images provide unequivocal confirm-ation of the hydrogel coating surrounding the GNS particle cores. We note, however, that slightly smaller hydrogel diameters were observed in the TEM images compared to those obtained by FE-SEM (*vide supra*) and DLS (*vide infra*), perhaps due to the ultrahigh vacuum and strong electron beam used to collect the TEM data.

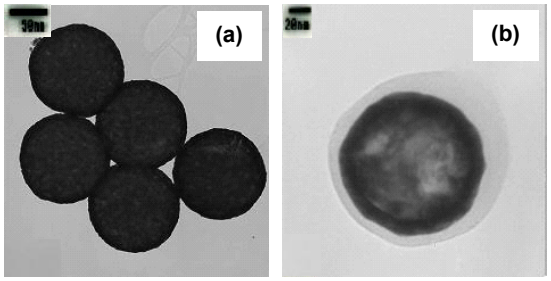

Figure 2. TEM images of (a) GNS particles (120 nm) and (b) hydrogel-coated GNS particles (160 nm).

Figure 3 presents the UV-vis absorption spectra of the THPC gold-seeded silica particles, GNS particles, and hydrogel-coated GNS particles. For the gold-seeded particles, the absorption maximum appears at 520-530 nm, which is characteristic of unaggregated small gold nanoparticles; in contrast, gold nanoshells are characterized by a broad absorption maximum ranging typically from 700 to 900 nm.[36] It is also known that the intensity and broadness of GNS absorption bands depend on the completeness and morphology of the gold coating on the silica particle cores.[37] Given the position, intensity, and broadness of the absorption bands centered at ~850 nm in Figure 3, we conclude that complete gold overlayers were grown on the silica particle cores.[9] Due

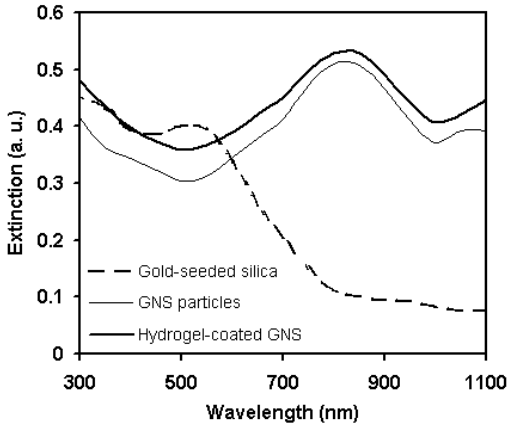

Figure 3. UV-vis spectra of THPC gold-seeded silica particles, GNS particles, and hydrogel-coated GNS particles under neutral pH conditions.

to the thinness of the hydrogel coating, the band position and intensity observed for the hydrogel-coated GNS particles are similar to those observed for the bare GNS particles (i.e., the hydrogel coating exerts no influence on the adsorption maximum). We note, however, a slight increase in band intensity at 300–600 nm for the hydrogel-coated GNS particles, arising perhaps due to enhanced scattering from the hydrogel matrix.

Using DLS and dilute neutral pH solutions, we observed systematic changes in the hydrodynamic diameter of hydrogel-coated GNS particles as a function of temperature; under these same conditions, the hydrodynamic diameter of bare GNS particles was invariant (Figure 4). Specifically, the diameter of bare GNS particles (~120 nm) remains constant as the temperature is altered between 25 °C and 45 °C, while the diameter of the hydrogel-coated GNS particles decreases by ~30 nm upon heating to 45 °C, but grows back to its original size upon cooling to 25 °C. The cooling and heating process was repeated several times and showed similar reversibility every time, providing indirect support for the presence of a poly(NIPAM) hydrogel coating on the GNS particles.[38–40] The collapse of the hydrogel polymers above the LCST arises from the loss of hydrogen bonding between water and hydrophilic sites on the hydrogel polymer backbone (i.e., between water and the backbone amide moieties).[38] Above the LCST, it has been proposed that the loss of hydrogen bonding between water and the amide backbone removes internal electrostatic repulsion within the hydrogel polymer matrix, leading to a collapse of the hydrogel superstructure.[38] The electrostatic environment can be fine-tuned by inserting ionizable groups, such as AAc and AAm moieties into the polymer backbone. The presence of additional hydrophilic sites along the polymer backbone enhances the water-swelling properties and thus increases the LCST.[39] For example, the LCST of pure poly(NIPAM) hydrogels is fixed at ~30 °C, but that of poly(NIPAM) hydrogels containing 5% AAc moieties is known to be higher, ranging from 34 to 40 °C.[38,40] It is important to note that the upper part of this temperature range is ideal for use in the human body, where the ambient temperature is 37 °C.

In a previous study of poly(NIPAM)-coated nano-particles in which the core consisted of a simple gold nanoparticle rather than a GNS particle,[41] we found that the incorporation of 5% AAc moieties led to a small increase in the LCST compared to that reported for free-standing co-poly(NIPAM) hydrogels.[38,40] This modest enhancement might arise from a decrease in the average interchain distance in hydrogel polymers that are anchored to metal nanoparticles.[41] In any event, appropriate tuning of the LCST can be accomplished simply by adjusting the content of AAc moieties in the co-polymer.[38,40]

As noted above, light at wavelengths ranging from 800–1200 nm can penetrate human skin and bone without harming the tissue.[42] As such, the hydrogel-coated GNS particles described here represent a unique thermo-responsive system that can be activated *in vivo*. Furthermore, impregnation of the hydrogel coatings with therapeutic agents (e.g., pharmaceuticals such as insulin or cisplatin) offer the possibility of targeted drug delivery that can be controlled optically.[43] Studies of drug loading and delivery using these nanoparticles are currently underway.

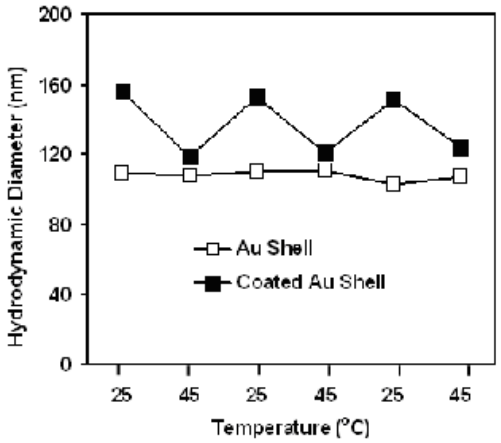

Figure 4. The hydrodynamic diameter of GNS particles and hydrogel-coated GNS particles as a function of alternating temperature.

IV. Conclusions

These studies have demonstrated the reliable preparation of GNS particles and the encapsulation of these particles within a thermo-responsive hydrogel matrix. Monodisperse GNS particles having diameters of ~120 nm and strong optical absorptions centered at ~850 nm were prepared. The individual GNS particles were then coated with a poly(NIPAM)-based haydrogel of variable thickness, ranging from ~20 nm to ~165 nm. While the thin coatings were readily grown on individual particles, the thicker coatings were more likely to encapsulate multiple GNS cores. The morphology, elemental composition, and properties of the composite nanoparticles were characterized by FE-SEM, EDX, TEM, and UV-vis spectroscopy. These data collectively demonstrate the formation of discrete hydrogel polymer-coated GNS particles. Analysis by DLS revealed that the hydrodynamic diameters of the hydrogel-coated GNS particles decrease with an increase in temperature from 25 to 40 °C, but then reversibly swell to their original size upon cooling back to 25 °C. As a whole, the composition and physical characteristics of these unique nanoparticles appear to be ideally suited for nanoscale drug delivery.

Acknowledgment

We are grateful for financial support from the Army Research Office, the National Science Foundation (ECS-0404308), the Texas Center for Superconductivity, and the Robert A. Welch Foundation (Grant E-1320). The use of the DLS was made possible by a grant from the Department of Energy to Professor Simon Moss (UH). We also thank Dr. I. Rusakova for assistance with the TEM measurements and Dr. J. C. Reina for assistance with the DLS measurements.

REFERENCES

[1] Kim, F.; Song, J. H.; Yang, P. *J. Am. Chem. Soc*. **2002**, *124*, 14316.

[2] Sun, Y.; Mayers, B.; Xia, Y. *Nano Lett.* **2003**, *3*, 675.

[3] Hao, E.; Kelly, K. L.; Hupp, J. T.; Schatz, G. C. *J. Am. Chem. Soc.* **2002**, *124*, 15182.

[4] Graf, C.; Blaaderen, A. V. *Langmuir* **2002**, *18*, 524.

[5] Link, S.; El-Sayed, M. A. *J. Phys. Chem. B* **1999**, *103*, 8410.

[6] Kelly, K. L.; Coronado, E.; Zhao, L. L; Schatz, G. C. *J. Phys. Chem. B* **2003**, *107*, 668.

[7] Cao, Y.–W.; Jin, R.; Mirkin, C. A. *J. Am. Chem. Soc.* **2001**, *123*, 7961.

[8] Oldenburg, S. J.; Jackson, J. B.; Westcott, S. L.; Halas, N. J. *Appl. Phys. Lett.* **1999**, *75*, 2897.

[9] Oldenburg, S. J.; Averitt, R. D.; Westcott, S. L.; Halas, N. J. *Chem. Phys. Lett.* **1998**, *288*, 243.

[10] Averitt, R. D.; Westcott, S. L.; Halas, N. J. *J. Opt. Soc. Am. B* **1999**, *16*, 1824.

[11] Averitt, R. D.; Sarkar, D.; Halas, N. J. *Phys. Rev. Lett.* **1997**, *78*, 4217.

[12] Simpson, C. R.; Kohl, M.; Essenpreis, M.; Cope, M. *Phys. Med. Biol.* **1998**, *43*, 2465.

[13] Gorelikov, I.; Field, L. M.; Kumacheva, E. *J. Am. Chem. Soc.* **2004**, *126*, 15938.

[14] Pelton, R. *Adv. Coll. Interface Sci*. **2000**, *85*, 1.

[15] Jeong, B.; Bae, Y. H.; Lee, D. S.; Kim, S. W. *Nature* **1997**, *388*, 860.

[16] Bergbreiter, D. E.; Case, B. L.; Liu, Y. S.; Caraway, J. W. *Macromolecules* **1998**, *31*, 6053.

[17] Schild, H. G.; Tirrell, D. A. *J. Phys. Chem.* **1990**, *94*, 4352.

[18] Saunders, B. R.; Vincent, B. *J. Chem. Soc. Faraday Trans*. **1996**, *92*, 3385.

[19] Zhou, S.; Chu, B. *J. Phys. Chem. B* **1998**, *102*, 1364.

[20] Winnik, F. M. *Polymer* **1990**, *31*, 2125.

[21] Jones, C. D.; Lyon, L. A. *Macromolecules* **2000**, *33*, 8301.

[22] Snowden, M. J.; Tomas, D.; Vincent, B. *Analyst* **1993**, *118*, 1367.

[23] Jones, C. D.; Lyon, L. A. *Macromolecules* **2003**, *36*, 1988.

[24] Zhu, M.–Q.; Wang, L.-Q.; Exarhos, G. J.; Li, A. D. Q. *J. Am. Chem. Soc.* **2004**, *126*, 2656.

[25] Pelton, R. H.; Pelton, H. M.; Morphesis, A.; Rowell, R. L. *Langmuir* **1989**, *5*, 816.

[26] Snowden, M. J.; Chowdhry, B. Z.; Vincent, B.; Morris, G. E.; *J. Chem. Soc. Faraday Trans.* **1996**, *92*, 5013.

[27] Priest, J. H.; Murray, S. L.; Nelson, R. J.; Hoffman, A. S. *Reversible Polym. Gels. Rel. Syst.* **1987**, *350*, 255.

[28] Yoshida, R.; Sakai, K.; Okano, T.; Sakuri, Y. *J. Biomater. Sci., Polym. Edn.* **1994**, *6*, 585.

[29] Saunders, B. R.; Vincent, B. *Adv. Coll. Interface Sci.* **1999**, *80*, 1.

[30] Saunders, B. R.; Crowther, H. M.; Vincent, B. *Macromolecules* **1997**, *30*, 482.

[31] Neyret, S.; Vincent, B. *Polymer* **1997**, *38*, 6129.

[32] Stöber, W.; Fink, A.; Bohn, E. *J. Colloid Interface Sci.* **1968**, *26*, 62.

[33] Waddell, T. G.; Leyden, D. E.; DeBello, M. T. *J. Am. Chem. Soc.* **1981**, *103*, 5303.

[34] Duff, D. G.; Baiker, A.; Edwards, P. P. *Langmuir* **1993**, *9*, 2301.

[35] Duff, D. G.; Baiker, A.; Gameson, I.; Edwards, P. P. *Langmuir* **1993**, *9*, 2310.

[36] Westscott, S. L.; Oldenburg, S. J.; Lee, T. R.; Halas, N. J. *Langmuir* **1998**, *14*, 5396.

[37] Charnay, C.; Lee, A.; Man, S.; Moran, C. E.; Radloff, C.; Bradley, R. K.; Halas, N. J. *J. Phys. Chem. B* **2003**, *107*, 7327.

[38] Shibayama, M.; Mizutani, S.; Nomura, S. *Macromolecules* **1996**, *29*, 2019.

[39] Kato, E. *J. Chem. Phys.* **1997**, *106*, 3792.

[40] Tan, K. C.; Wu, X. Y.; Pelton, R. H. *Polymer* **1992**, *33*, 436.

[41] Kim, J.–H.; Lee, T. R. *Chem. Mater.* **2004**, *15*, 4169.

[42] Sershen, S. R.; Westcott, S. L.; Halas, N. J.; West, J. L. *J. Biomed. Mater. Res.* **2000**, *51*, 293.

[43] Kim, J.–H.; Lee, T. R. *Drug Dev. Res.* **2006**, *67*, 61.